J|A|C|S
COMMUNICATIONS

Published on Web 09/26/2003

An Experimental Look into Subelectron Charge Flow

Roie Yerushalmi,[†] Kim K. Baldridge,[‡] and Avigdor Scherz*,[†]

Department of Plant Sciences, The Weizmann Institute of Science, 76100 Rehovot, Israel, and Department of Chemistry, University of California at San Diego, La Jolla, California 92093

Received May 5, 2003; E-mail: avigdor.scherz@weizmann.ac.il

The prediction and measurement of charge distribution and fragmental charge flow between interacting chemical entities in complex environments is a major challenge and an urgent need for modern chemistry, biology, material sciences, and other rapidly developing molecular disciplines.[1] It encompasses information related to fundamental quantities such as the electronic chemical potential (μ_e) and hardness (η) of molecular fragments as well as their interactions with the surroundings. Advances in quantum mechanical (QM) methodologies, particularly the density functional theory (DFT),[2] and computational capabilities have enabled the detailed calculation of electronic structures and properties of large molecular systems and provide a rigorous counterpart to the more "intuitive" concepts, such as electronegativity, that have served chemists in the design of such systems for decades. However, at the very fundamental level, the concept of atomic or group charges in a molecule has not been uniquely formulated, because it is not rigorously defined within the QM postulates.[3−5] As a result, the judgment of the quality of computational predictions relies on the availability of high-precision experimental data and the interpretation of related experimental observables. Furthermore, the use of computational techniques as an aid in designing large and complex molecules is practically limited. These shortcomings underscore the importance of developing experimental tools for reliable monitoring and prediction of charge flow between molecular fragments.

Here, we demonstrate a novel experimental approach capable of monitoring charge distribution and fragmental charge flow between a chelated metal center and reversibly bound molecules. The experimental approach shown here utilizes the recently described "molecular potentiometer".[6] In the demonstrated setting, the metal probe is a Ni(II) atom, and the interacting ligand molecules are changed in a modular manner (Figure 1). This includes ligands that have been systematically modified in a specific position with different functional groups while the rest of the molecular structure remains unchanged, for example, in the series: 4-picoline (**5**), pyridine (**6**), 4-bromopyridine (**8**), and 4-cyanopyridine (**9**). The choice of a Ni(II) metal center allows the study of all possible coordination geometries (tetra-, penta-, and hexacoordinated) in a systematic manner, in contrast to [Pd(II)]- or [Co(II)]BChls, for example, where only the tetra- or pentacoordinated complexes, respectively, are observed in solution. [Ni]BChl was titrated with different ligand molecules in anhydrous acetonitrile. The resolved spectroscopic (UV−vis−NIR) band shifts of 16 [Ni]-BChl complexes (ΔEQ_y, ΔEQ_x, ΔEB_x, and ΔEB_y) with one and two axial ligands are listed in Table 1. The charge flow (ΔQ^o_M) between each ligand and the [Ni]BChl molecule was derived from the absorption spectra in solution as previously described.[6] The spectroscopic data reported here suggest that when using a particular metal center, for example, Ni(II), changes in ΔQ^o_M, because of different ligand molecules, can be accurately determined by measuring the energetic band shift of a single electronic transition (ΔEQ_x, Figure 1C).

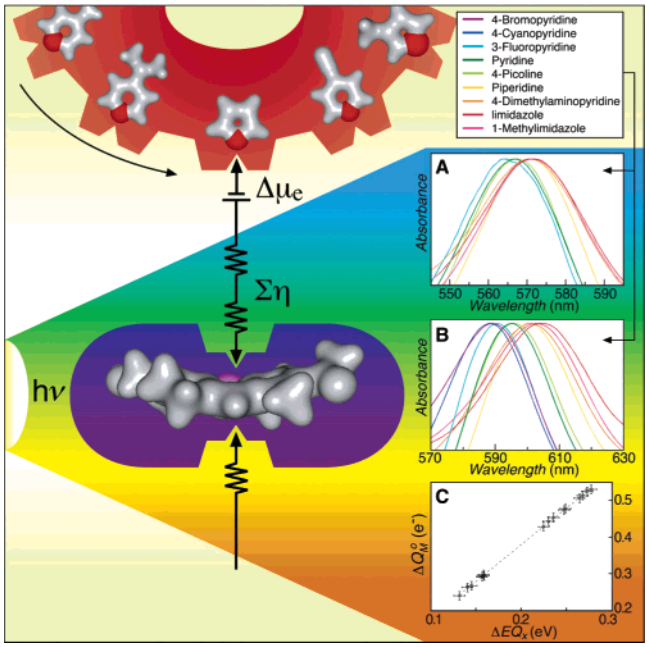

Figure 1. Binding of ligand molecules (gray and red molecules) to [Ni]-BChl changes the effective charge at the nickel metal center (violet).[7] This change consequently affects the orbital energies, via electrostatic interactions with the π electrons.[8] The orbital shifts are observed in the optical band transition energy shifts. The [Ni]BChl Q_x band shifts as a result of (A) one axial ligand, and (B) two axial ligands. The noncoordinated [Ni]BChl Q_x band (not shown) is located at 532 ± 1 nm. (C) The amount of charge flow (ΔQ^o_M) correlates linearly with the Q_x energetic band shift (ΔEQ_x); $R^2 > 0.99$.

This result is expressed through the linear correlation shown in Figure 1C, $\Delta Q^o_M = a^*\Delta EQ_x + b$, for the 16 complexes studied here.

Thus, additional spectroscopic contributions to ΔQ^o_M values that originate from changes in core size are constant (mainly reflected in the Q_y position[8]). This observation agrees with our computational data for the optimized structures of the nonligated low-spin [Ni]-BChl and the high-spin ($S = 1$) [Ni]BChl·L_n complexes. Following geometry optimization, charge analysis was performed for the set of 16 complexes to provide an independent computational determination of fragmental charge flow (ΔN_{Lig}, NPA).[9,10] Comparison of ΔQ^o_M and ΔN_{Lig} shows excellent correlation (Figure 2, □, $R^2 = 0.99$) for the entire data. Therefore, the Q_x band shift can be used for directly measuring the amount of charge transfer upon bond formation using the simple equation: $\Delta EQ_x = \alpha^*\Delta N_{lig}(\text{NPA}) + \beta$ (Figure 2, ○, $R^2 = 0.99$). The need for a scaling factor when comparing the experimental (ΔQ^o_M) and computational (ΔN_{Lig}, NPA) charge flow values reflects the experimental parameters and

[†] Weizmann Institute of Science.
[‡] University of California.

10.1021/ja035946y CCC: $25.00

Table 1. Summary of Experimental and Computational Results ([Ni]BChl·(L)$_n$ Indicates Mono- and Bi-ligated Complexes for n = (1,2), Respectively, and L = (1−9) Is a Ligand Molecule in the Following Order: Imidazole, 1-Methylimidazole, 4-(Dimethylamino)pyridine, Piperidine, 4-Picolone, Pyridine, 3-Fluoropyridine, 4-Bromopyridine, and 4-Cyanopyridine)

	spectroscopic band shifts[a]					NPA
complex	$-\Delta EB_y$ (eV)	$-\Delta EB_x$ (eV)	$-\Delta EQ_x$ (eV)	$-\Delta EQ_y$ (eV)	$-\Delta Q^o_M$[b] (e^-)	ΔN_{Lig}[d] (e^-)
[Ni]BChl·$(1)_1$	0.1574	0.00	0.1585	−0.0309	0.2977	0.1204
[Ni]BChl·$(2)_1$	0.1189	0.00	0.1587	−0.0252	0.2948	0.1223
[Ni]BChl·$(3)_1$	0.1381	0.00	0.1565	−0.0272	0.2928	0.1215
[Ni]BChl·$(4)_1$	0.1357	0.00	0.1565	−0.0281	0.2920	0.1355
[Ni]BChl·$(5)_1$	0.1123	0.00	0.1452	−0.0295	0.2672	0.1106
[Ni]BChl·$(6)_1$	0.1543	0.00	0.1404	−0.0334	0.2630	0.1105
[Ni]BChl·$(7)_1$	0.1437	0.00	0.1316	−0.0438	0.2400	0.1036
[Ni]BChl·$(1)_2$	0.2769	0.00	0.2774	−0.0354	0.5305	0.2303
[Ni]BChl·$(2)_2$	0.2806	0.00	0.2729	−0.0321	0.5246	0.2318
[Ni]BChl·$(3)_2$	0.2799	0.00	0.2677	−0.0342	0.5139	0.2241
[Ni]BChl·$(4)_2$	0.2659	0.00	0.2643	−0.0334	0.5059	0.2227
[Ni]BChl·$(5)_2$	0.2712	0.00	0.2488	−0.0347	0.4779	0.2137
[Ni]BChl·$(6)_2$	0.2676	0.00	0.2471	−0.0354	0.4739	0.2115
[Ni]BChl·$(8)_2$[c]	0.2686	0.00	0.2355	−0.0330	0.4541	0.2039
[Ni]BChl·$(7)_2$	0.2740	0.00	0.2299	−0.0349	0.4437	0.2000
[Ni]BChl·$(9)_2$[c]	0.2236	0.00	0.2247	−0.0305	0.4286	0.1975

[a] Spectroscopic components of mono- and bi-ligated species were resolved using factor analysis techniques as published elsewhere.[6] [b] Determined from the spectroscopic band shifts using the loading coefficients given by Noy et al.[8] [c] Only the bi-ligated species were observed in solution. [d] Computationally determined positive partial charge on axial ligand(s) employing the NPA charge analysis at the B3P86/SDD level of theory.

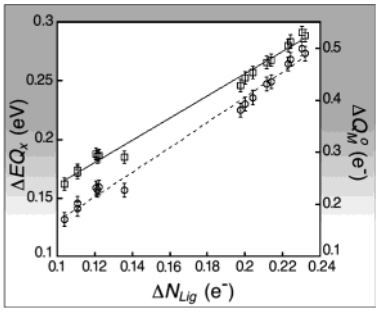

Figure 2. Computationally determined charge transfer (ΔN_{Lig}) versus experimental data. Each point in the graphs corresponds to a [Ni]BChl·L$_n$ complex listed in Table 1. The x coordinate of the graph corresponds to the amount of calculated charge, ΔN_{Lig}, transferred by the axial ligand(s) using (A) the NPA analysis as implemented in Gaussian 98.[13] The left y coordinate represents the spectroscopic band shift, ΔEQ_x (○), and the right y coordinate is the charge transfer, ΔQ^o_M (□), as previously described.[6,8] There is considerable agreement ($R^2 = 0.99$) between experimentally derived values and the NPA analysis.

level of theory used in the frame of the experimental model and QM calculations, respectively. This issue is the subject of current study.

Exploring the correlation of different computational approaches and the experimental results, as demonstrated here, provides a straightforward assessment of various charge schemes. Applying this type of analysis, for example, to the widely used Mulliken analysis, reveals that it fails to reproduce the experimental data. The poor performance of the Mulliken analysis for the determination of partial charges as compared with more advanced methods is well-documented in the literature.[11,12] Nevertheless, Mulliken charges, as well as charges derived from other computational schemes that suffer from fundamental limitations, are still widely used today. We believe that this is the result of the lack of an experimental approach that provides an independent and direct measure for such properties, as presented here.

The experimental monitoring of fragmental charge flow for a sufficiently large set of chemical entities (atoms in molecules, functional groups, and whole molecules) together with theoretical concepts such as the electronegativity equalization principle (EEP)[14] are expected to provide the effective values of different electronic indices such as μ_e, η, and higher electronic moments. Notably, the measured values are readily obtained for various environments and states of matter rather than the gas phase. Recent synthetic advances in BChl chemistry[15] are expected to enable the incorporation of modified [M]BChls as molecular probes in self-assembled monolayers (SAMs), as well as in synthetic and natural proteins.[16]

Acknowledgment. This research was supported by a US-Israel Binational Science Foundation grant (9800323), a Sonder-Forschungsbereich grant (533), the Willstatter-Avron-Minerva Foundation for Photosynthesis, and the NIH NBCR (RR08605-06). A grant for supercomputer time was provided through the NPACI NRAC program, and the Israeli HPCU program. A.S. is an incumbent of the Yadelle and Robert Sklare Chair for Biochemistry. We wish to acknowledge the SDSC-ROCKS team for hardware support on the SDSC-meteor cluster running ROCKS.

References

(1) (a) Simon, N. T.; Richard, G. D.; Maria-Teresa, M. A.; Donald, H. *Nature* **1995**, *373*, 228−230. (b) Matthew, R. H.; Enrico, A. S.; Donald, H.; Ian, A. W. *Science* **1994**, *263*, 646−652. (c) Rodriguez, J. A.; Goodman, D. W. *Science* **1992**, *257*, 897−903. (d) Zhang, P.; Crespi, V. H.; Chang, E.; Louie, S. G.; Cohen, M. L. *Nature* **2001**, *409*, 69−71. (e) Wang, T.; Moll, N.; Cho, K.; Joannopoulos, J. D. *Phys. Rev. Lett.* **1999**, *82*, 3304−3307. (f) Fujiwara, A.; Takahashi, Y. *Nature* **2001**, *410*, 560−562.

(2) Hohenberg, P.; Kohn, W. *Phys. Rev.* **1964**, *B136*, 864.

(3) Bader, R. F. W. *Atoms in Molecules*, 1st ed.; Clarendon Press: Oxford, 1994.

(4) Sigfridsson, E.; Ryde, U. *J. Comput. Chem.* **1998**, *19*, 377−395.

(5) Chermette, H. *J. Comput. Chem.* **1999**, *20*, 129−154.

(6) Noy, D.; Yerushalmi, R.; Brumfeld, V.; Ashur, I.; Scheer, H.; Baldridge, K. K.; Scherz, A. *J. Am. Chem. Soc.* **2000**, *122*, 3937−3944.

(7) According to the EEP, charge flow between interacting chemical systems is driven by the initial difference in the electronic chemical potential, $\Delta\mu e$, and restrained by the sum of the hardness, $\sum\eta$.

(8) Noy, D.; Fiedor, L.; Hartwich, G.; Scheer, H.; Scherz, A. *J. Am. Chem. Soc.* **1998**, *120*, 3684−3693.

(9) All structures considered here were optimized using DFT methods (B3P86/SDD) and were followed by NPA charge analysis as implemented in Gaussian 98, revision A.7.

(10) Reed, A. E.; Weinstock, R. B.; Weinhold, F. *J. Chem. Phys.* **1985**, *83*, 735−746.

(11) Politzer, P.; Mulliken, R. S. *J. Chem. Phys.* **1971**, *55*, 5135−5136.

(12) Wiberg, K. B.; Hadad, C. M.; Breneman, C. M.; Laidig, K. E.; Murcko, M. A.; LePage, T. J. *Science* **1991**, *252*, 1266−1272.

(13) Frisch, M. J.; Trucks, G. W.; Schlegel, H. B.; Scuseria, G. E.; Robb, M. A.; Cheeseman, J. R.; Zakrzewski, V. G.; Montgomery, J. A., Jr.; Stratmann, R. E.; Burant, J. C.; Dapprich, S.; Millam, J. M.; Daniels, A. D.; Kudin, K. N.; Strain, M. C.; Farkas, O.; Tomasi, J.; Barone, V.; Cossi, M.; Cammi, R.; Mennucci, B.; Pomelli, C.; Adamo, C.; Clifford, S.; Ochterski, J.; Petersson, G. A.; Ayala, P. Y.; Cui, Q.; Morokuma, K.; Malick, D. K.; Rabuck, A. D.; Raghavachari, K.; Foresman, J. B.; Cioslowski, J.; Ortiz, J. V.; Stefanov, B. B.; Liu, G.; Liashenko, A.; Piskorz, P.; Komaromi, I.; Gomperts, R.; Martin, R. L.; Fox, D. J.; Keith, T.; Al-Laham, M. A.; Peng, C. Y.; Nanayakkara, A.; Gonzalez, C.; Challacombe, M.; Gill, P. M. W.; Johnson, B. G.; Chen, W.; Wong, M. W.; Andres, J. L.; Head-Gordon, M.; Replogle, E. S.; Pople, J. A. *Gaussian 98*, revision A.7; Gaussian, Inc.: Pittsburgh, PA, 1998.

(14) Sanderson, R. T. *Chemical Bonds and Bond Energy*; Academic Press: New York, 1976.

(15) Yerushalmi, R.; Ashur, I.; Scherz, A. In *Metal-substituted Bacteriochlorophylls: Novel Molecular Tools*; Scheer, H., Ed.; 2003, in press.

(16) Noy, D. Private communication. Recently, [M]BChl derivatives were successfully incorporated into synthetic water-soluble proteins, forming stable complexes.

JA035946Y